

6-9-2017

High-Frequency Dissolved Organic Carbon and Nitrate Measurements Reveal Differences in Storm Hysteresis and Loading in Relation to Land Cover and Seasonality

M. C. H. Vaughan

W. B. Bowden

J. B. Shanley

A. Vermilyea

R. Sleeper

See next page for additional authors

Follow this and additional works at: https://digitalcommons.uri.edu/nrs_facpubs

Citation/Publisher Attribution

Vaughan, M. C. H., et al. (2017), High-frequency Dissolved Organic Carbon and Nitrate Measurements Reveal Differences in Storm Hysteresis and Loading in Relation to Land Cover and Seasonality. *Water Resour. Res.*, 53, 5345–5363, doi:10.1002/2017WR020491
Available at: <http://dx.doi.org/10.1002/2017WR020491>

This Article is brought to you by the University of Rhode Island. It has been accepted for inclusion in Natural Resources Science Faculty Publications by an authorized administrator of DigitalCommons@URI. For more information, please contact digitalcommons-group@uri.edu. For permission to reuse copyrighted content, contact the author directly.

High-Frequency Dissolved Organic Carbon and Nitrate Measurements Reveal Differences in Storm Hysteresis and Loading in Relation to Land Cover and Seasonality

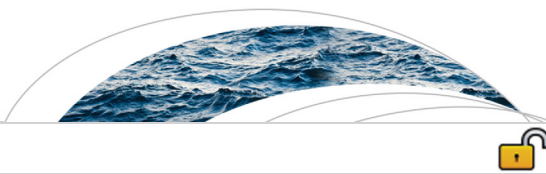
Creative Commons License



This work is licensed under a [Creative Commons Attribution-Noncommercial-No Derivative Works 4.0 License](https://creativecommons.org/licenses/by-nc-nd/4.0/).

Authors

M. C. H. Vaughan, W. B. Bowden, J. B. Shanley, A. Vermilyea, R. Sleeper, Arthur J. Gold, Soni M. Pradhanang, S. P. Inamdar, D. F. Levia, A. S. Andres, F. Birgand, and A. W. Schroth



RESEARCH ARTICLE

10.1002/2017WR020491

Special Section:

Continuous Nutrient Sensing in Research and Management: Applications and Lessons Learned Across Aquatic Environments and Watersheds

Key Points:

- An improved hysteresis index revealed remarkable variation in storm dynamics for 126 storms in watersheds with varied land use/land cover
- Seasonality influenced storm nitrate loading; interactions between farm practices and seasonal dynamics were captured by sensors
- Sites had generally anticlockwise storm hysteresis for DOC, though storm nitrate hysteresis direction varied by land use/land cover

Supporting Information:

- Supporting Information S1

Correspondence to:

M. C. H. Vaughan,
matthew.vaughan@uvm.edu

Citation:

Vaughan, M. C. H., et al. (2017), High-frequency dissolved organic carbon and nitrate measurements reveal differences in storm hysteresis and loading in relation to land cover and seasonality, *Water Resour. Res.*, 53, 5345–5363, doi:10.1002/2017WR020491.

Received 27 JAN 2017

Accepted 4 JUN 2017













Accepted article online 9 JUN 2017

Published online 2 JUL 2017

© 2017. The Authors.

This is an open access article under the terms of the Creative Commons Attribution-NonCommercial-NoDerivs License, which permits use and distribution in any medium, provided the original work is properly cited, the use is non-commercial and no modifications or adaptations are made.

High-frequency dissolved organic carbon and nitrate measurements reveal differences in storm hysteresis and loading in relation to land cover and seasonality

M. C. H. Vaughan¹ , W. B. Bowden¹ , J. B. Shanley² , A. Vermilyea³ , R. Sleeper¹ , A. J. Gold⁴ , S. M. Pradhanang⁴ , S. P. Inamdar⁵ , D. F. Levia⁵ , A. S. Andres⁵ , F. Birgard⁶ , and A. W. Schroth¹ 

¹University of Vermont, Burlington, Vermont, USA, ²U.S. Geological Survey, Montpelier, Vermont, USA, ³Castleton University, Castleton, Vermont, USA, ⁴University of Rhode Island, Kingston, Rhode Island, USA, ⁵University of Delaware, Newark, Delaware, USA, ⁶North Carolina State University, Raleigh, North Carolina, USA

Abstract Storm events dominate riverine loads of dissolved organic carbon (DOC) and nitrate and are expected to increase in frequency and intensity in many regions due to climate change. We deployed three high-frequency (15 min) in situ absorbance spectrophotometers to monitor DOC and nitrate concentration for 126 storms in three watersheds with agricultural, urban, and forested land use/land cover. We examined intrastorm hysteresis and the influences of seasonality, storm size, and dominant land use/land cover on storm DOC and nitrate loads. DOC hysteresis was generally anticlockwise at all sites, indicating distal and plentiful sources for all three streams despite varied DOC character and sources. Nitrate hysteresis was generally clockwise for urban and forested sites, but anticlockwise for the agricultural site, indicating an exhaustible, proximal source of nitrate in the urban and forested sites, and more distal and plentiful sources of nitrate in the agricultural site. The agricultural site had significantly higher storm nitrate yield per water yield and higher storm DOC yield per water yield than the urban or forested sites. Seasonal effects were important for storm nitrate yield in all three watersheds and farm management practices likely caused complex interactions with seasonality at the agricultural site. Hysteresis indices did not improve predictions of storm nitrate yields at any site. We discuss key lessons from using high-frequency in situ optical sensors.

1. Introduction

Storms transport considerably more carbon and nutrients to receiving water bodies than during times of base flow [Inamdar et al., 2006; Fellman et al., 2009]. Understanding fluxes during storm events is critical since storms in the U.S. are expected to increase in frequency and intensity in the future [Walsh et al., 2014]. Storms are difficult to characterize with traditional “grab sampling” approaches because they are ephemeral in time and variable in space. The development of in situ optical sensors has revolutionized water quality monitoring and gives researchers an improved view into the important and dynamic role that storms play in water quality. These instruments have several advantages over traditional hand or automatic grab sampling to characterize storms, including (1) subhourly measurement intervals to resolve rapid changes in water quality; (2) no need for hazardous chemicals to analyze solute concentrations; (3) no storage or transportation issues that can impact lab analyses of grab samples; and (4) the ability to continuously monitor streamwater chemistry so that rare and episodic events can be characterized. Assessing solute export using in situ sensors also reduces error associated with discharge based load estimations, since discharge-solute relationships can break down during extreme precipitation events or due to variable event-based hysteresis loops [Dhillon and Inamdar, 2013].

Recently, in situ spectrophotometers have been used to measure streamwater dissolved organic carbon (DOC) and nitrate (NO₃⁻) concentrations, two important water quality characteristics. DOC is transported from terrestrial sources of carbon to receiving water bodies [Prairie, 2008], attenuates ultraviolet radiation that is harmful to microorganisms [Morris et al., 1995; Bukaveckas and Robbins-Forbes, 2000], affects metal pollutant transport and bioavailability [Driscoll et al., 1988; Ravichandran, 2004], and has been identified as the primary cause of harmful trihalomethane disinfectant byproduct formation during drinking water

treatment [Reckhow and Singer, 1990; Chow et al., 2007; Kraus et al., 2008; Nguyen et al., 2013]. Nitrate is an essential nutrient to aquatic ecosystems; however, when supply exceeds ecosystem demand, elevated concentrations in surface waters cause numerous adverse effects on downstream freshwater ecosystems [Smith et al., 1999; Camargo and Alonso, 2006], including changes in the biotic community structure and loss of biodiversity [Pardo et al., 2011], eutrophication [Smith et al., 1999], increased acidification in forested systems [Driscoll et al., 2001] leading to increased mobilization of toxic aluminum [Baker et al., 1996], and deterioration of drinking water supply quality [Townsend et al., 2003]. Therefore, in situ high-frequency measurements of these key parameters have exciting potential to inform our understanding of a diverse suite of water quality issues operating across multiple spatial and temporal scales.

Quantifying the dynamic relationship between solute concentration and stream discharge can improve understanding of solute transport pathways and active source areas [e.g., Evans and Davies, 1998; House and Warwick, 1998; Chanut et al., 2002]. Hysteresis occurs when the concentration-discharge relationship differs on the rising limb of a storm versus the falling limb [e.g., Johnson and East, 1982; Bowes et al., 2015]. When a solute has higher concentrations on the rising limb versus the falling limb, a plot of these parameters forms a clockwise loop. This nonlinear relationship is often the result of an exhaustible solute supply that is close to the measurement location [e.g., Bowes et al., 2009]. When concentrations are higher on the falling limb versus the rising limb, an anticlockwise hysteresis pattern emerges. This occurs when sources are more distal, have a longer transport time, stem from deeper subsurface zones, or a combination of these factors [Donn et al., 2012; Bierozza and Heathwaite, 2015]. Hysteresis relationships can provide some indication of the general sources of solutes during storms, though it is not clear whether hysteresis dynamics correlate with solute loading.

Seasonal effects can have significant influences on storm DOC and nitrate export. During spring snowmelt, high water table levels activate upper organic soil horizons during storms, causing greater export of DOC, especially from riparian soils [Boyer et al., 1997; Raymond and Saiers, 2010]. This is also a season in which nitrate export loads tend to be higher because nitrate stored in the snowpack is transported to the stream during rain-on-snow events, and biological uptake has not yet begun [Driscoll et al., 2003]. In the summer months, stream water DOC loads tend to decrease because lower precipitation and drier soils result in fewer storms that activate flow paths in upper soil horizons that leach DOC. Stream water nitrate concentrations also tend to fall at this time as biological uptake increases dramatically [Likens, 2013].

Land use/land cover (LULC) also plays a key role in determining the amount of DOC and nitrate that is exported during storms. Studies in small agricultural watersheds often note elevated base flow DOC concentrations relative to other streams in the same region and increases in DOC concentration during storm events [Dalzell et al., 2005; Royer and David, 2005; Vidon et al., 2008; Saraceno et al., 2009] because agricultural activities alter the source of stream water DOC and lead to greater in-stream DOC production due to greater fertility [Wilson and Xenopoulos, 2008; Stanley et al., 2012]. A significant portion of nitrogen delivered to water bodies during storms is from nonpoint sources, stemming from agricultural practices and atmospheric deposition due to human activities [Boyer et al., 2002]. Agriculture and urban land use change have been shown to contribute to increased nitrate loads in streams [Boesch et al., 2001] and can alter the storm response of a watershed from supply-limited, typical of a forested stream, to a transport-limited condition [Rosenzweig et al., 2008; Carey et al., 2014]. Urbanization often has a substantial impact on stream hydrology [Walsh et al., 2005] and can result in elevated organic carbon loading in streams [Sickman et al., 2007; Newcomer et al., 2012]. Increased DOC loads in urban streams during storms can be sourced from wastewater inputs [Sickman et al., 2007; Aitkenhead-Peterson et al., 2009], organic material deposited onto impervious surfaces, human and animal waste, and grass clippings from home lawns, all combined with greater hydrologic response [Sickman et al., 2007]. These numerous sources are in addition to decomposing organic matter that accumulates in soil layers, as in unaltered systems. Even so, there is no consensus on the overall effects of urbanization on DOC concentrations and loads. Studies suggest that urbanization causes DOC export to either increase [Kaushal and Belt, 2012], decrease [Kominoski and Rosemond, 2011], or provide a compensatory mechanism where internal production balances decrease of external inputs, resulting in no net change [Parr et al., 2015].

The Northeast Water Resources Network (NEWRnet) was created in Spring 2014 to better understand water quality dynamics in the Northeast U.S. by using emerging optical water quality sensor technology. Our sensor array provided an excellent resource to see how several of the factors summarized above influence

storm DOC and nitrate dynamics. Continuous monitoring in the spring, summer, and fall seasons over 19 months using in situ spectrophotometers allowed us to quantify DOC and nitrate storm exports using high-frequency measurements. We use these data to address the following research objectives: (1) evaluate the use of in situ spectrophotometers to quantify DOC and nitrate storm hysteresis and exports using high-frequency measurements in streams with varied LULCs; (2) compare intrastorm DOC and nitrate hysteresis relationships between watersheds of differing LULCs to determine differences in source areas and solute transport processes; (3) compare the influence of agricultural, urban/suburban, and forested LULCs on storm DOC and nitrate exports; and (4) determine what factors, including hysteresis, might explain the variance in storm DOC and nitrate exports. Through these analyses, we develop a more holistic perspective of how land use, seasonality, and storm event water yield impact storm event loading and the temporal evolution of water chemistry during storms.

2. Study Areas

We compared streams draining watersheds with various primary LULCs to characterize the influence of LULC on storm hysteresis and exports of DOC and nitrate. The study sites were in the Lake Champlain Basin of Vermont in the Northeastern U.S. (Table 1 and Figure 1). Hungerford Brook is a primarily agricultural catchment, including dairy, row crops, hay, and pasture. Potash Brook is situated near the city of Burlington, Vermont's densest population center. Its watershed is primarily characterized by urban and suburban development (54%), though there is some agricultural and forest cover (29% and 11%, respectively). The Wade Brook catchment is primarily forested (95%) and is situated on the western slope of Vermont's Green Mountain chain. Hungerford Brook and Wade Brook eventually drain to the Missisquoi River and Lake Champlain; Potash Brook drains directly to Lake Champlain. Precipitation totals in the Wade Brook catchment are higher than the catchments of Hungerford Brook and Potash Brook due to orographic effects (Table 1).

3. Methods

3.1. In Situ Measurements

We used s::can Spectrolyser UV-Vis spectrophotometers (s::can Messtechnik GmbH, Vienna, Austria) in each stream, deployed from June 2014 to December 2015 for spring, summer, and fall seasons. The sensors were housed in PVC tubing for protection during high flows, were solar powered for autonomous operation, and transmitted data in real time through a cellular data network. The spectrophotometers measure light absorbance at wavelengths ranging from 220 to 750 nm at 2.5 nm increments and were programmed to take measurements every 15 min. Optical path lengths were either 5 or 15 mm, depending on the typical turbidity of each stream (Table 1), and absorbance spectra were normalized by optical path length for comparison. Sensor measurement windows were automatically cleaned before each measurement with a silicone wiper and cleaned manually in the field at least every 2 weeks using pure ethanol. To focus on dissolved constituents, absorbance spectra were corrected for the effects of turbidity by fitting a third-order polynomial in the visible range of the spectrum, extrapolating into the UV portion, and then subtracting the extrapolated absorbance from the raw spectrum [Langergraber *et al.*, 2003; Avagyan *et al.*, 2014]. Discharge measurements were acquired from a U.S. Geological Survey gaging station where available (Hungerford Brook Station 04293900), or calculated from discharge-depth rating curves developed with velocity-area calculations [Turnipseed and Sauer, 2010], salt dilutions [Moore, 2005], and 15 min stage measurements using atmospherically compensated pressure transducers.

3.2. Lab Measurements

Manual grab samples were collected during base flow and storms to compare and calibrate in situ absorbance spectrophotometer measurements to laboratory measurements. A total of 226 grab samples were taken over the duration of this study. Each sample was filtered using rinsed glass fiber GF/F filters (nominal pore size of 0.7 μm) into new HDPE bottles. Samples were stored on ice in the field, then DOC samples were stored in a cooler at 2°C (for DOC samples), and nitrate samples were stored in a freezer at -23°C until analysis. Lab DOC measurements were made using a Shimadzu TOC-L analyzer using the combustion catalytic oxidation method. Lab nitrate-N measurements were made using the QuickChem method 31-107-04-1E on a Lachat analyzer.

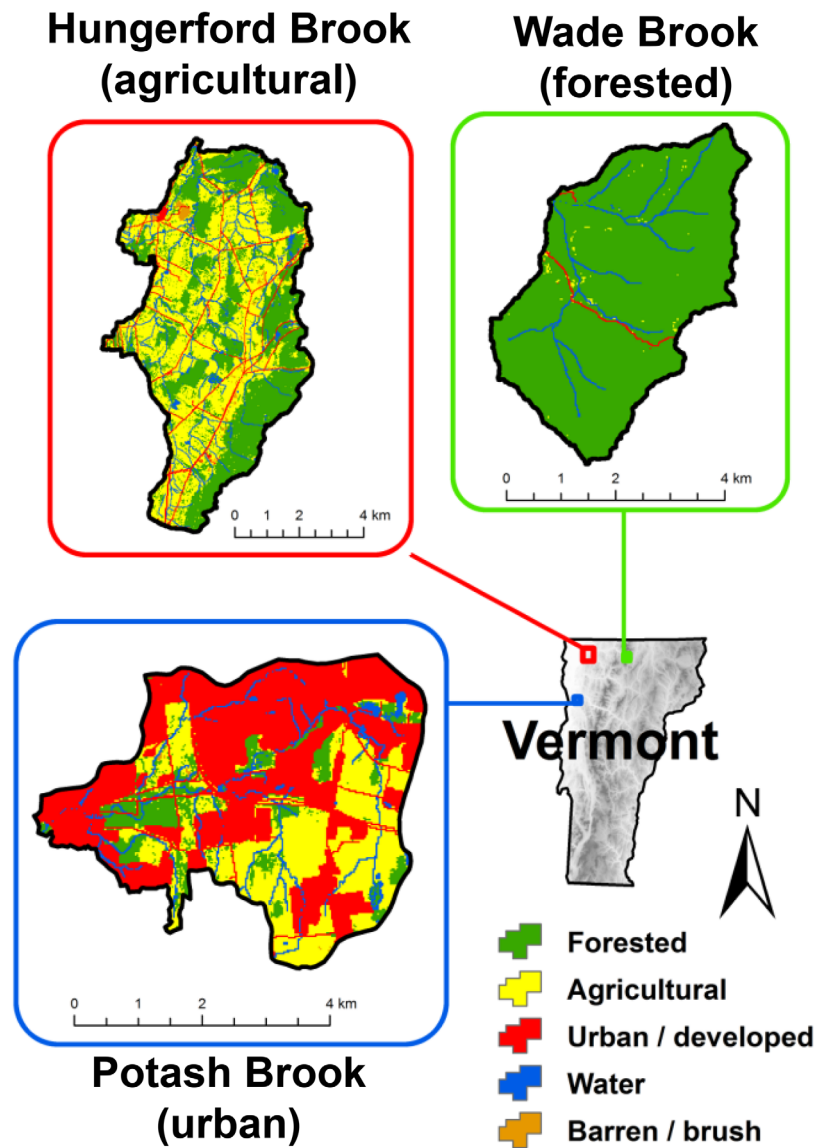


Figure 1. Map showing location and land use/land cover of the three study areas.

3.3. Preparation of In Situ Sensor Data

Because of the high dimensionality of absorbance spectra, dimension reduction combined with multiple regression techniques have proven effective in recent studies to predict DOC and nitrate concentrations [Avagyan *et al.*, 2014; Etheridge *et al.*, 2014]. We used an identical approach to Etheridge *et al.* [2014], where partial least squares regression is employed with the pls package in R to generate calibration algorithms [Mevik *et al.*, 2016; R Core Team, 2015]. To validate calibrations, we ensured that a randomly chosen subset representing 10% of each calibration data set could be adequately predicted using the remaining data. Once validated, the full data set was used for each calibration. Spectral slope ratio [Helms *et al.*, 2008] was calculated for all grab samples and compared among sites to determine how DOC character might influence calibrations. Spectral slope was calculated using the equation:

$$a_{\lambda} = a_{\lambda_{ref}} e^{-S(\lambda - \lambda_{ref})}, \quad (1)$$

where S is the best fit spectral slope (nm^{-1}), a is the Napierian absorption coefficient (m^{-1}), λ is wavelength (nm), and λ_{ref} is the reference wavelength (285 nm). The spectral slope ratio was then found by dividing the spectral slope over the 275–295 nm range by the spectral slope in the 350–400 nm range.

Table 1. Summary of Study Area Characteristics

	Hungerford Brook	Potash Brook	Wade Brook
Primary land cover	Agricultural	Urban/suburban	Forest
Watershed area (km ²)	48.1	18.4	16.7
Percentage forested	40.5	10.6	95.1
Percentage agricultural	44.8	29.1	0.6
Percentage urban	5.6	53.5	0.8
Percentage impervious area	2.3	23.9	0.0
Sensor elevation (m)	80	42	320
Maximum watershed elevation (m)	354	143	981
Mean watershed slope (%)	5.6	5.3	26
Mean air temperature (°C)	6.7	7.8	4.2
Mean precipitation (mm yr ⁻¹)	1000	961	1453
Mean annual atmospheric nitrogen deposition (kg N km ⁻²)	450	340	570
Sensor optical path length used (mm)	5.0	5.0	15.0
Coordinates (WGS 1984)	44.918403°N, 73.055664°W	44.444331°N, 73.214482°W	44.864468°N, 72.552904°W
Soil and surficial geology	Sandy, silty, and stony loams	Sandy and silty loams, clay	Glacial till, sandy loam
Vegetation	Agricultural, mixed northern hardwoods and conifer	Urban/suburban landscaping, mixed northern hardwoods and conifer, agricultural	Mixed northern hardwoods and conifer

Time series of DOC and nitrate-N concentration (mg L⁻¹) were generated using each calibration, and short data gaps (<2 h) were filled using cubic spline interpolation to produce a continuous data set for the analyzed storms. We then multiplied predicted concentration by concurrent discharge (m³ s⁻¹) to estimate DOC and nitrate-N load (g s⁻¹).

Storms were delineated by base flow separation using the filter method outlined in *Arnold et al.* [1995]. This filtering approach partitions the streamflow hydrograph into base flow and direct runoff components. A minimum rise criterion determined the start of each storm and the end of the storm was chosen manually as a point on the falling limb where storm event discharge approached antecedent or interevent levels (Figure 2). Manual selection of the inflection point was used since we found that analyses were not sensitive to minor differences in the designated ending point of the storm.

Geographic separation of sites and differences in hydrologic response for each watershed resulted in differing numbers of observed storms for each site.

3.4. Calculation of Hysteresis Indices

We used a recently improved hysteresis index to quantify temporal solute concentration dynamics for each storm and compare across our sites [*Lloyd et al.*, 2016]. This hysteresis index is based on normalized discharge and storm solute concentrations, as follows:

$$Q_{i,norm} = \frac{Q_i - Q_{min}}{Q_{max} - Q_{min}}, \quad (2)$$

$$C_{i,norm} = \frac{C_i - C_{min}}{C_{max} - C_{min}}, \quad (3)$$

where Q_i and C_i are the discharge and solute concentration

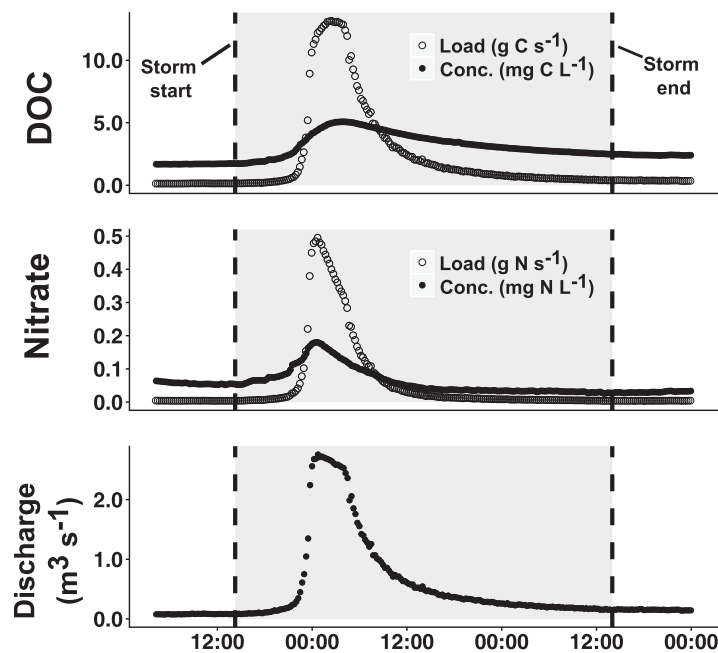


Figure 2. Plot of high-frequency (15 min) data from a storm at the forested site on 4–6 October 2014. DOC and nitrate concentrations were measured with the six:can spectrophotometer and load was calculated by the product of concentration and concurrent discharge. The shaded region between the dashed lines shows the period of the record that was considered for this storm; the DOC and nitrate loads were integrated over this period, and then divided by watershed area to determine storm DOC and nitrate yield.

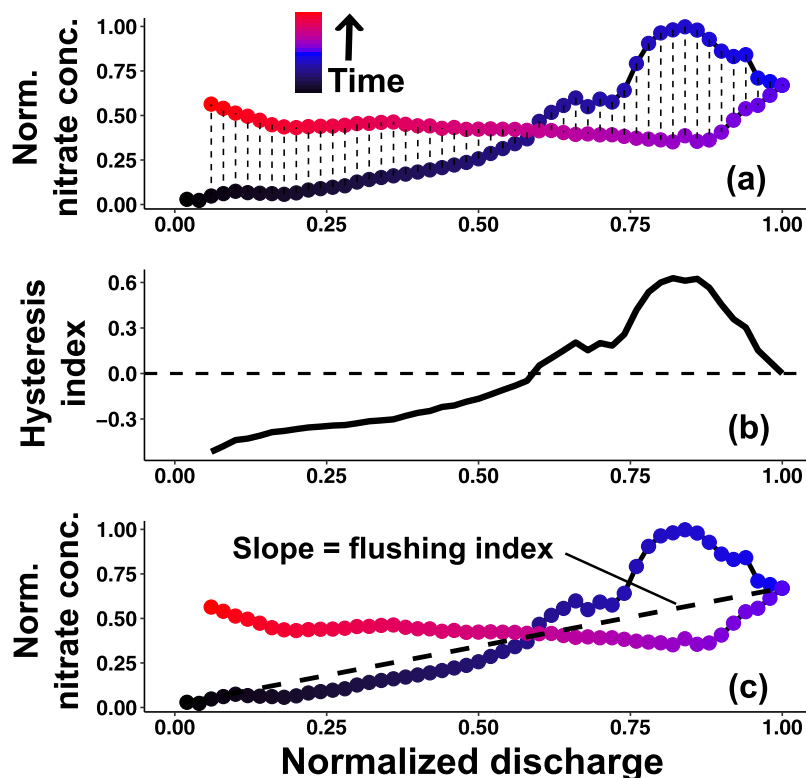


Figure 3. Plot of (a) normalized nitrate concentration versus normalized discharge, (b) hysteresis index, and (c) flushing index illustration for a storm at the agricultural site on 30 September to 2 October 2015. We calculated hysteresis index HI_j by subtracting the normalized solute concentration on the falling limb from that of the rising limb for each 2% of normalized discharge, and the storm hysteresis HI is the mean of these values. Flushing index FI is the slope of the line that intersects the normalized solute concentration at the beginning and at the point of peak discharge of the storm. For this storm, nitrate $HI = -0.03$ and $FI = 0.64$.

values at time step i , Q_{max} and Q_{min} are the maximum and minimum discharge values in the storm, and C_{max} and C_{min} are the maximum and minimum solute concentrations in the storm. Then, we found an interpolated solute concentration C_j by linear regression of $C_{i,norm}$ at 2% intervals of $Q_{i,norm}$ on both the rising and falling limbs at interval j using two adjacent measurements. The hysteresis index at each discharge interval was determined by subtracting the falling limb from the rising limb:

$$HI_j = C_{j,rising} - C_{j,falling} \quad (4)$$

HI_j was only calculated for intervals where data existed for both rising and falling limbs because not all storms returned to their initial discharge condition. An overall hysteresis index for each storm event was determined by calculating the mean of all HI_j values (Figures 3a and 3b). This value is conveniently scaled from -1 to 1 , where negative values indicate anticlockwise hysteresis, positive values indicate clockwise hysteresis, and the magnitude of HI indicates the amount of difference between the rising and falling limbs. We compared these measures using the nonparametric Kruskal-Wallis test for differences in the medians [Kruskal and Wallis, 1952], and Levene's test for equality of variances among sites [Levene, 1960].

Storms were further characterized using a flushing index FI similar to the one used by Butturini *et al.* [2008]:

$$FI = C_{Q_{peak,norm}} - C_{initial,norm} \quad (5)$$

where $C_{Q_{peak,norm}}$ and $C_{initial,norm}$ are the normalized solute concentrations at the point of peak discharge and the beginning of the storm, respectively. This index also conveniently ranges from -1 to 1 , where negative values indicate a diluting effect on the rising limb, and positive values indicate an increase in concentration, or "flushing" effect on the rising limb. FI values are equal to the slope of the line that intersects the first normalized solute concentration measured in a storm and the normalized solute concentration at peak discharge (Figure 3c).

3.5. Statistical Analyses for Storm Nitrate and DOC Yield

For each storm, we integrated DOC and nitrate-N load from the beginning to the end of the event to determine export mass (kg) of each solute. This was divided by watershed area to calculate DOC and nitrate-N yield (kg km^{-2}) for comparison among sites. We also integrated discharge for each storm to calculate the amount of runoff and then divided by watershed area to determine water yield (mm). The ratio of storm DOC yield to water yield ($\text{kg C km}^{-2} \text{mm}^{-1}$), and the ratio of storm nitrate yield to water yield ($\text{kg N km}^{-2} \text{mm}^{-1}$) were also calculated for each storm. The nonparametric Kruskal-Wallis test was employed to detect significant differences in population medians [Walford, 2011].

To explore the relationship between both storm DOC yield and water yield, and storm nitrate yield and water yield, least squares linear regression was performed for each, grouped by site. When less than 90% of variance was explained, additional regressions were performed by grouping storms by season. Since storm DOC and nitrate yields are calculated using stream discharge, they are intrinsically autocorrelated with storm water yield. This means that if solute concentration is constant, we would expect a perfectly linear correlation. A weak correlation is indicative of greater variability in solute concentration that is related to other factors besides stream discharge. Difference in correlation coefficients between sites stems from differences in solute concentrations during and among storms.

Regression coefficients between these subgroups were tested for statistically significant differences using the equation:

$$Z = \frac{b_1 - b_2}{\sqrt{SE_1^2 + SE_2^2}}, \quad (6)$$

where b_1 and b_2 are the regression coefficients of each model, and SE_1 and SE_2 are the associated standard errors [Paternoster et al., 1998]. Models with regression coefficients that were not significantly different were then tested for categorical differences using analysis of covariance (ANCOVA). For this test and all others in the paper, we used $p \leq 0.05$ as significant.

4. Results

4.1. Sensor Performance

The partial least squares regression technique used sensor absorbance spectra to predict nitrate-N concentrations with excellent comparison to lab measured values. More than 99% of the variance in laboratory measured concentrations was explained by sensor predictions at all three sites, with a standard error of $\pm 0.0078 \text{ mg N L}^{-1}$ (Figure 4a).

Spectral slope ratios of grab samples were significantly different among sites ($p < 0.0001$) (Figure 5), and calibrations to predict DOC concentrations were optimal when data were grouped by site (Figures 4b–4d). The sensors explained 96%, 95%, and 97% of the variance in lab measured DOC concentrations at the agricultural, urban, and forested sites, respectively. The standard error was highest at the agricultural site with a value of $\pm 0.045 \text{ mg C L}^{-1}$ and was lowest at the forested site with a value of $\pm 0.025 \text{ mg C L}^{-1}$.

4.2. Storm DOC Hysteresis

We observed 126 storms, including 40 at the agricultural site, 26 at the urban site, and 60 at the forested site (supporting information Figure S1). The DOC hysteresis loop pattern varied greatly from storm to storm, and the median DOC hysteresis index was negative for all three sites, indicating a typical anticlockwise loop pattern (Figure 6a). The median DOC hysteresis indices were not significantly different among sites, though the variances were significantly different among sites by Levene's test ($p = 0.013$). The agricultural stream had the highest variance in DOC hysteresis index ($\sigma^2 = 0.09$), which was more than double that of the urban and forested sites ($\sigma^2 = 0.04$ for each).

Plotting DOC storm hysteresis index versus DOC storm flushing index revealed that most storms at all three sites increased in concentration on the rising limb and had falling limbs that were even higher in concentration than the rising limb. There was notable variability in this relationship for all three sites (Figure 6c). We found no apparent patterns relating storm DOC hysteresis or flushing index to seasonal or other measured variables.

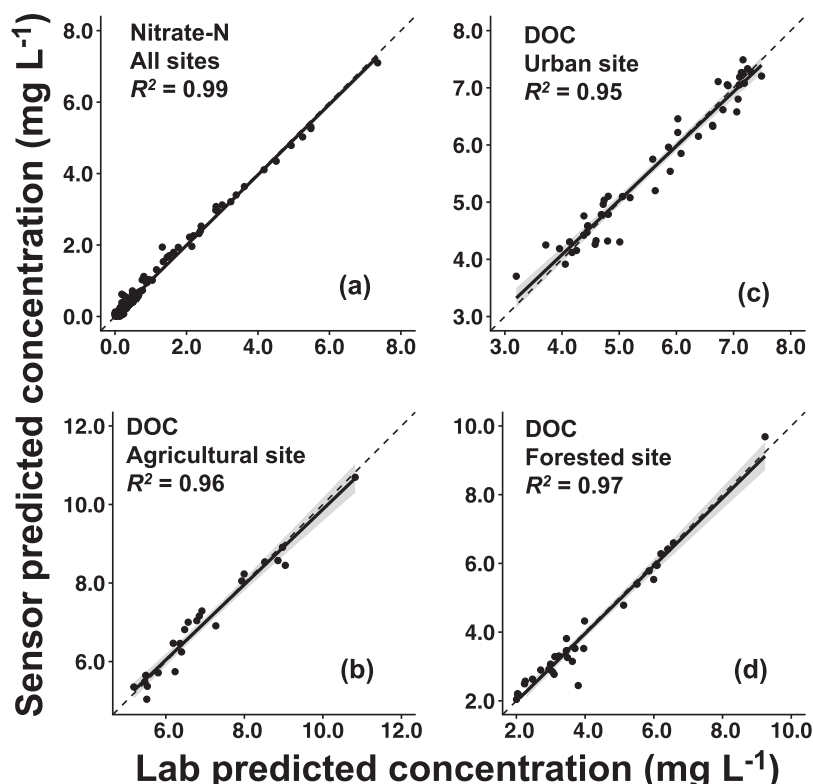


Figure 4. Plots of sensor predicted (a) nitrate and (b–d) DOC concentrations versus lab measured values. Shaded regions indicate 95% confidence intervals. The partial least squares calibration algorithm causes all regression lines to assume the equation $y = x$, and the dashed line is 1:1. All relationships were highly significant ($p < 0.0001$).

4.3. Storm Nitrate Hysteresis

The nitrate hysteresis analysis for the 126 storms revealed differences among the sites. The median nitrate hysteresis indices were negative for the agricultural site (anticlockwise loop pattern), positive (clockwise loop pattern) for the urban and forested sites, and were significantly different by the Kruskal-Wallis test ($p < 0.0001$). The forested site had a higher positive median hysteresis index than the urban site, indicating larger clockwise loop patterns (Figure 6b). The agricultural stream had the highest variance in nitrate hysteresis index ($\sigma^2 = 0.15$) and was 2–3 times higher than variances for the urban and forested sites ($\sigma^2 = 0.05$ and 0.08 , respectively).

Plotting nitrate storm hysteresis index versus nitrate storm flushing index revealed remarkable variability among sites. Most storms at the urban and forested streams showed decreasing nitrate concentrations on the rising limbs, and even lower nitrate concentrations on the falling limbs. The agricultural stream showed greater variability than the others though tended toward clockwise hysteresis and negative flushing index, or

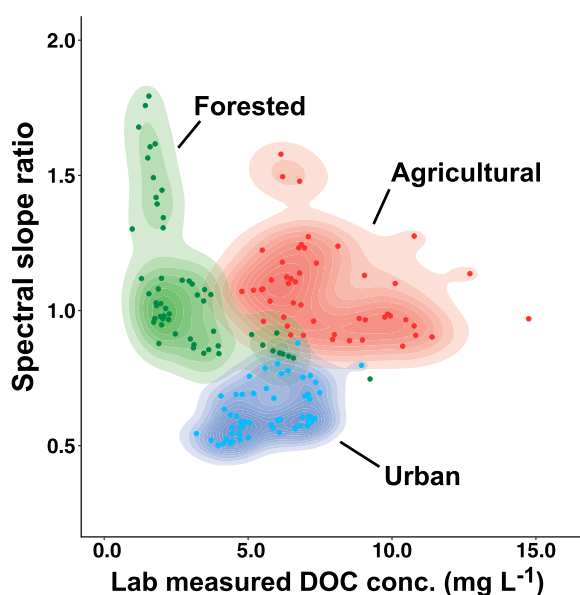


Figure 5. Plot of spectral slope ratio versus lab measured DOC concentration. Shaded areas show high density regions for each site.

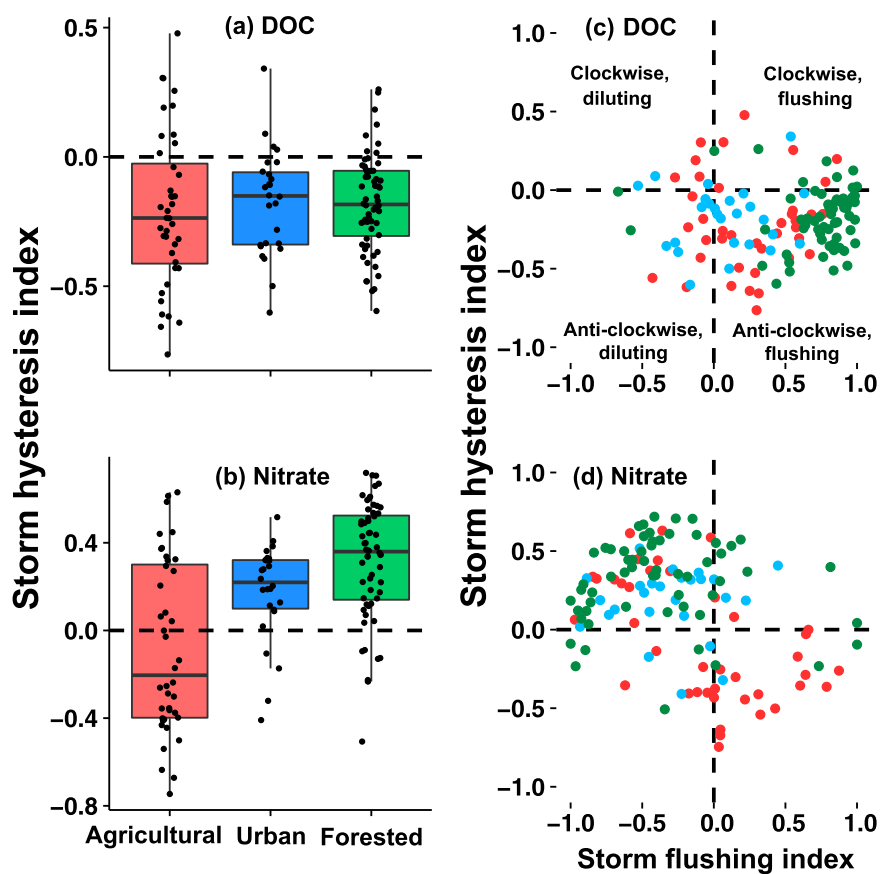


Figure 6. Box and whisker plots of storm hysteresis indices for (a) DOC and (b) nitrate, and plots of storm hysteresis index versus storm flushing index at the agricultural (red), urban (blue), and forested (green) sites for (c) DOC and (d) nitrate.

anticlockwise hysteresis and positive flushing index (Figure 6d). We found no apparent patterns relating storm nitrate hysteresis or flushing index to seasonal or other measured variables.

4.4. Storm DOC Yield

The median ratio of storm DOC yield to water yield was statistically different at each site, as revealed by a Kruskal-Wallis test ($p < 0.0001$). The highest median ratio is at the agricultural ($8.39 \text{ kg C km}^{-2} \text{ mm}^{-1}$), followed by the urban ($5.37 \text{ kg C km}^{-2} \text{ mm}^{-1}$), and is lowest at the forested site ($2.98 \text{ kg C km}^{-2} \text{ mm}^{-1}$). Water yield alone explains a large portion of the variance in storm DOC yield for each of the three monitored sites. With respect to DOC yield per storm water yield, the agricultural stream was largest, followed by the urban and finally the forested streams. By equation (6), differences in slope are statistically significant between the agricultural and the other two sites ($p < 0.0001$), but not between the urban and forested sites ($p = 0.16$) (Figure 7a). The lack of a significant difference in slope qualifies these sites for an ANCOVA test, which reveals that there is a statistically significant difference in the relationship between storm DOC yield and storm water yield for the urban and forested stream.

4.5. Storm Nitrate Yield

The median ratio of storm nitrate yield to water yield is statistically different at each site, as revealed by a Kruskal-Wallis rank sum test ($p < 0.0001$). The highest median ratio is at the agricultural ($2.52 \text{ kg km}^{-2} \text{ mm}^{-1}$), followed by the urban ($0.27 \text{ kg km}^{-2} \text{ mm}^{-1}$), and is lowest at the forested site ($0.12 \text{ kg km}^{-2} \text{ mm}^{-1}$). Among the three sites, a large portion of the variance in storm nitrate yield can be explained at the agricultural site with storm water yield through linear regression ($R^2 = 0.77$). However, only 53% and 14% of the variance can be explained by storm water yield for the urban and forested sites, respectively (Figure 7b).

In general, the agricultural site exports higher storm nitrate yield per water yield than the urban site, and the forested site exports the lowest amount of storm nitrate yield per storm water yield of the three. Differences

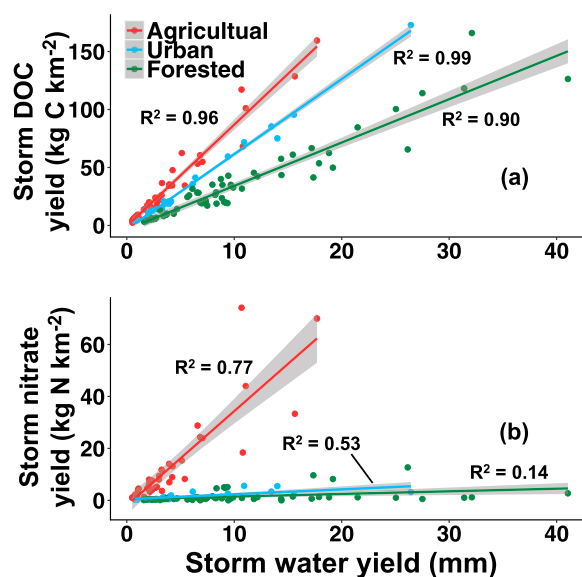


Figure 7. Plot of (a) storm DOC yield versus storm water yield and (b) storm nitrate yield versus storm water yield for all 126 storms observed during the 2014–2015 field seasons. Shaded regions indicate 95% confidence intervals. For storm DOC yield, relationships were highly significant for each site ($p < 0.0001$), and hypothesis tests comparing the sites showed significant differences between each site. For storm nitrate yield, the agricultural site had a significantly steeper slope than the forested and urban sites, and no significant differences were apparent between the urban and forested sites.

in storm nitrate yield among sites became more pronounced with increased storm water yield. The regression slopes between the agricultural and urban sites, and between the agricultural and forested sites were significantly different by equation (6) ($p < 0.0001$). The difference in regression slopes for the urban and forested stream were not significant, however ($p = 0.076$), and an ANCOVA test showed no significant difference between the regressions ($p = 0.39$).

4.6. Seasonal Effects on Storm Nitrate Yield

At the agricultural site, a larger portion of the variance in storm nitrate yield could be explained by storm water yield when the storms were grouped by spring, summer, and fall seasons. In addition, the regression slope coefficient between storm nitrate yield and storm water yield was significantly greater for summer than spring storms ($p < 0.0001$), greater for summer than fall storms ($p = 0.016$), and greater for fall storms than spring storms ($p = 0.024$) by equation (6) (Figure 8a).

A larger portion of the variance in storm nitrate yield at the urban site could be explained by storm water yield when grouped by season (Figure 8b). Equation (6) also revealed that the regression slope at the urban site was significantly higher for spring storms than summer storms ($p = 0.027$), but not significantly different between other storms. This qualified these subgroups for an ANCOVA test, which revealed that there is a significant categorical difference between spring and fall storms ($p < 0.0001$). The ANCOVA test showed no significant differences between summer and fall storms at the urban site.

Grouping storms by season at the forested site showed a significant difference in regression slopes between spring storms and the other two seasons ($p < 0.0001$), though not between summer and fall storms (Figure 8c) ($p = 0.14$), and the ANCOVA test showed no significant categorical difference between summer and fall storms.

Plotting the ratio of storm nitrate yield to water yield for each storm reveals that there are large differences among sites and that seasonal trends differ (Figure 9). At the agricultural site, this ratio increases through the spring, decreases through the summer, then increases once again in the fall. While swings in this ratio are less pronounced at the urban site, there is a decrease through the spring, the ratio stays low in the summer, then increases again in the fall. At the forested site, this ratio is by far highest in the early spring, then decreases throughout the year.

5. Discussion

5.1. Effects of Land Use/Land Cover on Optical Sensor Calibrations

This study is the first to apply UV-Vis spectrophotometry to determine DOC and nitrate concentrations in agricultural, urban, and forested catchments in the same region, and lessons learned in utilizing these sensors may be applicable to others who wish to monitor water quality parameters in a variety of settings at a high frequency. The Ocean Spectrolyser sensors provided accurate and precise in situ UV-Vis spectra, though we found that local calibrations for DOC and nitrate based on our own lab analyses performed better than the “global calibration” algorithms provided by the vendor (supporting information Figure S2). The partial

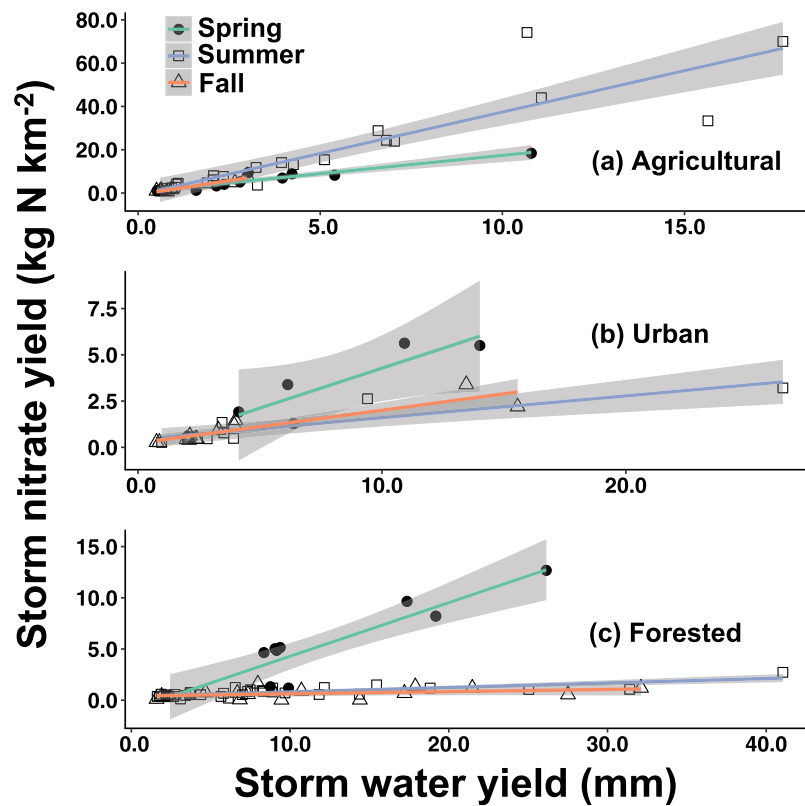


Figure 8. Plots of storm nitrate yield versus water yield grouped by season for the (a) agricultural, (b) urban, and (c) forested streams. Shaded regions indicate 95% confidence intervals.

least squares regression calibration technique was successful in using the high dimensional UV-Vis spectra to predict DOC and nitrate concentrations in a variety of conditions (Figures 4a–4d), so we recommend using this approach.

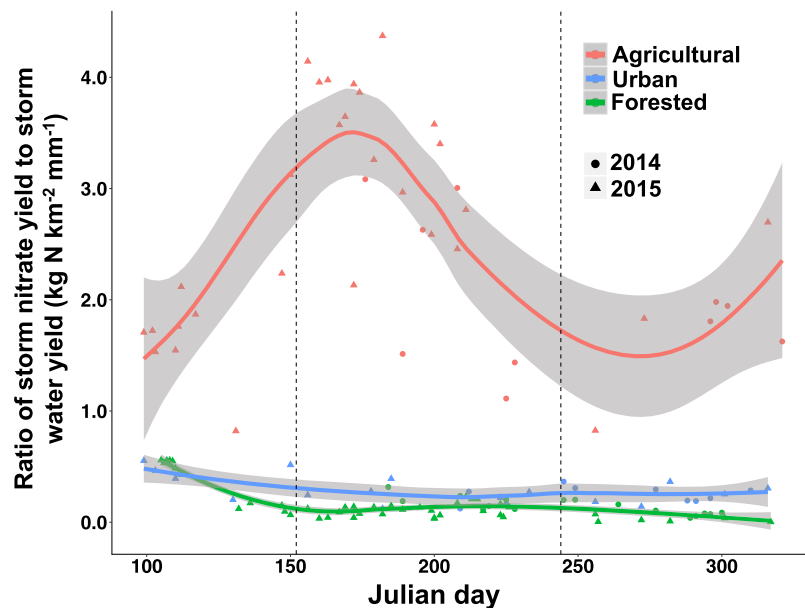


Figure 9. Plot of the ratio of storm nitrate yield to storm water yield versus the Julian day that the storm started. Lines were created with high-order polynomial regression. Shaded regions indicate 95% confidence intervals. One outlier was removed from plot for clarity, but remained for analyses (Agricultural, Julian day 152, 6.9 kg N km⁻² mm⁻¹).

Nitrate concentrations were predicted well in all sites using one common algorithm generated by partial least squares regression, despite differences in optical properties of stream water between sites (Figure 4a). This is not surprising since the nitrate molecule consistently absorbs UV light near $\lambda = 220$ nm [Johnson and Coletti, 2002]. In contrast, significant differences in DOC pool composition among sites did necessitate site-specific DOC calibrations. The DOC pool likely represents thousands of molecules absorbing light in the UV-Vis spectrum [Stubbins et al., 2014], and diversity in the composition of this pool can influence the calibration used to predict DOC concentration from UV-Vis absorbance spectra. Agricultural and urban land uses have been shown to influence DOC character [e.g., Wilson and Xenopoulos, 2009], and the spectral slope ratio, a proxy that is inversely related to molecular weight, was significantly different among the sites (Figure 5). In addition, studies measuring DOC export character in a variety of land use conditions have found that aromatic and humic content increases significantly during storms [Saraceno et al., 2009; Inamdar et al., 2011; Yoon and Raymond, 2012]. It is therefore quite likely that both cross-site differences (due to LULC) and intrasite variability (due to shifts in DOC sources during storm events) in DOC composition necessitated individual calibrations at each site. These issues are likely broadly applicable and should be considered by any investigator seeking to study storm event DOC dynamics using this technology.

Calibrations were also affected by the method of sample collection. Automated programmable pump samplers (e.g., ISCO samplers) are popular as a means to collect water samples remotely when researchers are not able to be in the field. However, we found that including samples from automated samplers resulted in lab results that were less reliable for calibration purposes. This impact was more pronounced for DOC than for nitrate (supporting information Figure S3). We suspect that this effect may be due to unstable storage temperature and the variable amount of time between sample collection and filtration. If these challenges can be addressed with remote filtration and refrigerated storage, then perhaps automatic samplers could be useful in expanding calibration data sets for future studies.

5.2. Effects of Land Use/Land Cover on Storm DOC and Nitrate Hysteresis

This study applied the recently improved hysteresis index metric outlined by Lloyd et al. [2016] to DOC and nitrate dynamics for a large number of storms, and we calculated hysteresis indices at finer resolution than previously used (2% intervals of storm discharge). Hysteresis patterns for DOC and nitrate were highly variable (Figures 6a and 6b) and did not correlate with seasonal or other measured variables. The three sites exhibited high variability in storm DOC dynamics, though all sites showed generally similar storm DOC anticlockwise hysteresis and positive flushing behavior (Figure 6c). The positive flushing index suggests that proximal DOC sources are plentiful enough to increase streamwater concentration on the rising limb, while the anticlockwise loop pattern suggests that DOC concentrations are higher on the falling limb than the rising limb, and that distal sources of DOC are activated later in the storm as hydrologic pathways connect, and/or that transport time for DOC is greater than that of water in the stream channel. This finding differs from the findings of some small forested catchments [Buffam et al., 2001; Hood et al., 2006; Raymond and Saiers, 2010], though it is similar to results of other forested catchments [Moore and Jackson, 1989; Brown et al., 1999; McGlynn and McDonnell, 2003; Pellerin et al., 2012], and at least one study in an agricultural catchment [Morel et al., 2009]. The dynamics we observed fit well with the conceptual model described by McGlynn and McDonnell [2003]. They found that source waters shifted from riparian to hillslope waters during storm events, and that the rising concentrations from hillslope waters occurred as soil became sufficiently saturated to connect upslope sources to the stream. While our different sites have distinct upland sources of DOC, it appears that they all share a similar dynamic, in that these sources are likely distal and hydrologically connected to the stream later in the storm cycle. This is remarkable, considering the differing sources of DOC and hydrologic pathways among the three watersheds. Urban systems, for example, are heavily affected by sewers, ditches, gutters, and runoff from impervious surfaces [Kaushal and Belt, 2012]. Watershed DOC sources range from manure and residual crop matter in agricultural fields, to wetlands and upland organic soils in the forested catchment, to sewer bacterial communities and grass clippings in the urban stream, yet the relative timing of connectivity and possibly the mechanism for delivery is not significantly different among the three sites.

The agricultural watershed displayed high variability in storm nitrate hysteresis (Figure 6b), though tended toward an anticlockwise pattern. This pattern coupled with a positive flushing index for many storms (Figure 6d) suggests the transport of plentiful proximal sources early in storm cycles, followed by enrichment from distal and plentiful sources of nitrate. Others have attributed this pattern to the rise of the water table

to the upper horizons that store accumulated nitrate from fertilizer application [Oeurng *et al.*, 2010]. While differences in watershed characteristics may be a contributing factor in differing storm nitrate dynamics, soil nitrate enrichment from fertilizer application may be a primary driver. While results on nitrate hysteresis in agricultural areas reported by others vary, our results generally agree with many that also report anticlockwise nitrate hysteresis patterns [Van Herpe and Troch, 2000; Oeurng *et al.*, 2010; Outram *et al.*, 2014]. In contrast, Bowes *et al.* [2015] observed clockwise nitrate hysteresis for 21 out of 36 storms in an agricultural watershed in southern England. While this does not reflect the trend toward anticlockwise hysteresis behavior we observed, both this study and ours observed a high amount of variance in agricultural nitrate hysteresis behavior. Interestingly, Darwiche-Criado *et al.* [2015] also observed a wide variety of storm nitrate hysteresis patterns in an agricultural area in the Flumen River, Spain. Though agricultural practices in that region differ greatly from those of our study area, they identified possible linkages between fertilization and irrigation practices with hysteresis patterns.

The median nitrate hysteresis index at the forested site was positive (clockwise) and the flushing index was generally negative, which suggests a proximal nitrate supply that is quickly depleted from riparian soils [Creed and Band, 1998]. Others' observations vary on the direction of nitrate hysteresis found in forested streams. Studies find clockwise behavior [Zhang *et al.*, 2007], anticlockwise behavior [Buffam *et al.*, 2001; Rusjan *et al.*, 2008], and at times no consistent pattern [Andrea *et al.*, 2006]. Storms at our urban site also had a positive median nitrate hysteresis index and generally negative flushing index. To our knowledge, only one other study has investigated storm nitrate hysteresis in urban streams, in which case the stream exhibited clockwise nitrate hysteresis for 14 out of the 17 storms observed [Carey *et al.*, 2014], which is in agreement with the nitrate hysteresis pattern at our urban site. Any nitrate sources that have accumulated on impervious surfaces will quickly transport to the urban stream network due to artificially increased drainage density, in addition to nitrogen pools accumulated in riparian soils, as in the forested system. In both the urban and forested systems, the combination of general clockwise hysteresis and negative flushing index patterns suggest that distal nitrate sources are not plentiful enough, and/or do not hydrologically connect to the stream network sufficiently to increase streamwater concentrations at the point of measurement.

The breadth of our data set shows what is possible with continuous high-frequency water quality data and new methods to quantify storm hysteresis. However, the remarkable variability that we observed in intra-storm hysteresis dynamics within and across sites highlights the need for continuously monitoring many storms, since sampling error is likely when inferring hysteresis patterns and suggested biogeochemical processes if only a few storms are observed. This level of detail in hysteresis calculations and the emergence of optical sensor technology will allow for better hysteresis measurement and comparisons in the future, but the dramatic variability and unpredictable hysteresis trajectories when comparing 126 storms across LULC clearly illustrates that there is much work needed to understand what controls the behavior of solutes within specific storm events over time and space.

5.3. Effects of Land Use/Land Cover on Storm DOC Yield

The high proportion of the variance in storm DOC yield explained by water yield at our sites suggests that DOC flux is driven by storm water yield for each LULC and is not influenced by the exhaustibility of these source areas (Figure 7a). The wetting of soil columns during storms connects DOC source areas to streams, and this process of DOC delivery appeared to be similar among sites. However, we found statistically significant differences in storm DOC yield versus water yield relationships, indicating that LULC drives the relationship between storm DOC yield and water yield across these sites by essentially setting a concentration range for stormwater. This storm water concentration range is likely determined by the relative abundance, nature and connectivity of DOC sources within each catchment, which is impacted heavily by LULC. Other factors such as seasonality and the antecedent conditions we observed did not have a substantial impact on storm DOC yield. While storm water yield is known to be subject to shifts in seasonal patterns, the DOC that we expect to be exported at each site with a given water yield does not vary significantly in our study areas.

It has been established that human activities in agricultural areas alter the source of fluvial DOC and lead to greater autochthonous DOC production [Wilson and Xenopoulos, 2008; Stanley *et al.*, 2012], and the differences we observed in storm DOC yield between land uses are similar to what others have recently found

[e.g., Yoon and Raymond, 2012; Caverly et al., 2013]. Urban and suburban development has also been shown to alter sources of DOC [e.g., Sickman et al., 2007]. Our results also suggest that urban and suburban development increase the storm export of DOC over undeveloped forest land cover, which is similar to the findings of Kaushal and Belt [2012] in the city of Baltimore, Maryland. This increase has been attributed to increased hydrologic connectivity and greater drainage density following installations of underground pipe networks, gutters, and ditches [Elmore and Kaushal, 2008], and additional DOC sources not found in forested catchments, such as sewage, lawn clippings, and more prevalent algal communities [Kaushal and Belt, 2012].

5.4. Effects of Land Use/Land Cover and Seasonality on Storm Nitrate Yield

The relationships between storm nitrate yield and water yield suggest that LULC has a dramatic impact on storm nitrate yield in the study areas. Our results comparing agricultural to urban and forested LULC are consistent with others', as nitrate concentrations are often elevated in agricultural areas due to nitrogen amendment [Carpenter et al., 1998]. The regression slopes between storm nitrate yield and water yield were significantly different between the agricultural site and the other sites, suggesting that the effect of agricultural LULC on nitrate loads is enhanced by larger storms (Figure 7b). In addition to increasing nitrate loads through direct fertilizer application, agricultural practices also alter the hydrology of watersheds by influencing evapotranspiration, and by developing tile drainage, which bypasses potential nitrogen retention hotspots [Royer et al., 2006]. Agricultural tile drainage could potentially be a key driver for the higher nitrate yield in this system, as it forms direct pathways to transport leached nitrate to streams [Hatfield et al., 1998; Dinnes et al., 2002]. Tile drainage is currently unregulated in the study area and the precise extent is unknown, though extent estimates for the agricultural site range from 60 to 76% [Winchell et al., 2011].

Urbanization is known to cause an increase in nitrate loading due to the production of new nitrate sources, and the alteration of hydrologic pathways due to impervious surfaces that bypass nitrogen retention hotspots, such as wetlands and riparian zones [Groffman et al., 2002; Kaushal et al., 2008; Rosenzweig et al., 2008]. While the median ratios of storm nitrate yield to water yield were shown to be significantly different among sites, the slope of the correlation between the storm nitrate yield and water yield was not significantly different between the urban and forested sites (Figure 7b). Increased DOC concentrations in urban streams have also been shown to increase biological uptake and denitrification of nitrogen [Sivirichi et al., 2011; Kaushal and Belt, 2012], so although we might expect increased inputs of inorganic nitrogen to the urban stream, the altered DOC dynamics may create a compensatory mechanism to curb this impact.

Interestingly, the seasonal effects on the relationship of storm nitrate yield versus water yield caused opposing trends between the agricultural and the other two sites. Regression slopes at the agricultural stream ranked from highest to lowest in the summer, fall, and spring, respectively. At the urban and forested sites, the descending order of regression slopes was spring, fall, and summer (Figure 8). The seasonal fluctuations in the ratio of storm nitrate yield to water yield we observed at the agricultural site (Figure 9) may be a signature of agricultural land use practices interacting with seasonal dynamics. A winter ban on manure application is lifted annually on 1 April, leading to widespread application during the spring. During this time, the ratio of storm nitrate yield to water yield increased throughout the spring season and peaked just after the beginning of the summer season. This pattern may be affected by biological uptake from field crops, which likely begins to increase substantially at this time. Through the summer growing season, this ratio decreased; we suggest that this may be due to a decrease in fertilizer application to fields, while concurrent biological uptake continues. In addition, the groundwater flux is likely lower during this time, causing the thickness of the unsaturated zone to increase, and the temperature is seasonally higher—all leading to higher rates of biogeochemical cycling and longer retention times. The ratio eventually reached a second minimum following the beginning of the fall season. When harvest occurred and biological uptake slowed, the greater leaching potential may have caused the ratio to increase again into late fall. Fall storms are also likely to be influenced by increased hydrological connectivity due to wetter soils following lower crop transpiration, and by the common practice of late season manure application prior to the winter ban that begins on 15 December. Manure is often applied in the fall due to the availability of labor, favorable weather, and lower fertilizer prices [Dinnes et al., 2002], although the majority of the nitrogen applied at this time is lost through pathways other than crop production before the subsequent growing season [Sanchez and Blackmer, 1988].

The ratio of storm nitrate yield to water yield was generally lower at the forested stream, and the seasonal pattern differed from the other sites. The ratio was highest during the few spring snowmelt events we observed, which may be when a pulse of atmospherically deposited nitrate is released from the melting snow pack, as inferred by *Pellerin et al.* [2012] at the Sleepers River in Vermont. Decreases in this ratio throughout the spring may be due to increasing vegetative nitrogen uptake across the catchment with green-up, leaving less nitrate available to be transported during storm events. This downward trajectory continues into the fall season, and the very low values of this ratio in the fall may be due to low nitrate concentrations during the litterfall period. Studies have observed lower base flow nitrate concentrations during this time of year, which has been attributed to increased heterotrophic uptake and denitrification of in-stream nitrate following the leaching of labile DOC from leaves in streams [*Sobczak et al.*, 2003; *Goodale et al.*, 2009; *Webster et al.*, 2009; *Sebestyen et al.*, 2014]. Patterns in storm nitrate yield versus storm water yield in our studied forested catchment underscore the importance of atmospherically deposited nitrogen stored in forest snowpack and frozen soils released during spring storms, and the biological uptake of mineral nitrogen in the summer and fall which may lower the nitrate yield of storms.

5.5. Challenges and Recommendations for High-Frequency Storm Monitoring

This study combines emerging optical sensor technology with recently developed methods for characterizing storms, and sheds light on the large amount of variation and complexity possible in DOC and nitrate storm dynamics. Many studies previously documenting DOC and nitrate hysteresis were conducted using grab samples, and often only considered a few storms. Therefore, comparing our results to those with smaller sample sizes may be problematic due to the potential for sampling error, and limited storm coverage and scope.

There are differences in watershed characteristics between our study areas that may confound LULC comparisons. Agricultural and urban areas have developed on flat valleys in the Northeast U.S., while steep mountain catchments remain forested, largely due to the difficulty to develop them and greater distance from population centers. Differences in topography, surficial soils, and hydrologic pathways are likely to impact our results, though the magnitude of the difference between agricultural and other LULCs presented here is compelling evidence that a significant portion can be attributed to LULC. As in situ water quality sensors become more affordable and accessible, future studies that investigate the influence of LULC would benefit from deploying sensors across a wider variety of agricultural, urban, and forested systems.

Collecting continuous, high-frequency data was critical to the success of this study, though we encountered several challenges in maintaining sensors due to biological fouling, flood damage, vandalism, and wildlife tampering. Significant effort was required for regular site visits to ensure data quality, and for troubleshooting when hardware or software failed. Also, calibration results show that regular and storm grab samples were needed to validate in situ measurements, so sensors are not able to completely replace manual grab samples at this point. We make the following recommendations as lessons learned for future studies employing in situ sensors:

1. We recommend using manual grab samples in place of automatically pumped samples that are stored unfiltered and unrefrigerated. We found that samples from our automatic samplers made the comparison to UV-Vis absorbance spectra unreliable for DOC calibrations (supporting information Figure S3).
2. We recommend reinforcing submerged wires to protect from aquatic wildlife and flood damage.
3. Maintaining the cleanliness of the optical measurement windows and wiper mechanism is critical for obtaining reliable UV-Vis absorbance spectra. For the Ocean Spectrolyser, we found that cleaning with pure ethanol and deionized water worked well to clear biological fouling in most situations. A thorough cleaning every 2 weeks was usually sufficient, though more frequent cleaning was necessary when stream conditions fostered high rates of biological production.
4. We recommend a system design that transmits data remotely. This was extremely useful in order to monitor data in real-time, react promptly to problems, store data offsite, and even troubleshoot remotely. In our sensor installations, Campbell Scientific CR1000 dataloggers with modems and antennas allowed us to access measured data through cellular networks via a laptop or handheld device.
5. We relied on solar power, which generally worked very well. Power supply was an issue at times, especially when daylight hours decline in the late fall season. If relying on solar power, we recommend careful selection of solar panel array and battery storage, and thoughtful installation with full exposure to the

sun. A gridded power system could be ideal, though this would still necessitate a battery backup since storms are often when power grids fail.

6. While the Spectrolyser is field rugged, we recommend constructing a secondary housing unit for stream installation. We used large PVC piping and steel carriage bolts, which protected the sensors from damage during several large flood events, but also allowed water and sediment to pass through unobstructed. This housing was also secured to land-based anchors via a steel cable to prevent loss of equipment during the largest events. This safety line proved useful on several occasions.

6. Conclusions

High-frequency measurements allowed for a new hysteresis calculation method to be applied to 126 storms and provided highly accurate and precise solute yield estimates. We observed remarkable variability in DOC storm dynamics and general trends in storm DOC hysteresis were similar in general among the three sites despite distinct DOC sources and hydrologic pathways. In addition, we found that the amount and timing of nitrate delivery to streams during storms differed significantly among the LULCs. We attribute this to land use practices generating more distal and plentiful nitrate source areas in the agricultural system, while nitrate depletion from more proximal riparian sources is more common in the urban and forested systems. We observed several differences among our sites of varied LULCs for storm DOC and nitrate loading. Both storm DOC and nitrate yields were elevated in the agricultural stream, and seasonal patterns reflected the complex interaction of land use practices, biogeochemical cycling, and climatic drivers. We also found that larger storm size magnifies differences between all LULCs for storm DOC yield and for storm nitrate yield in the agricultural site compared to the others.

While future work should include monitoring more storms during years with varied hydrologic inputs, more study areas are needed to put these findings into a cohesive context. As in situ optical sensor technology becomes more widely used, we can expect the cost of obtaining and maintaining these instruments to drop significantly. By incorporating sites with varied degrees of each end-member LULC type, we could better isolate land use effects from other watershed characteristics. Also, coupling in situ sensors with terrestrial sensor networks may help to better characterize the spatial distribution and temporal dynamics of source areas for DOC and nitrate, and aid in interpretation of integrated watershed signals.

Acknowledgments

This material is based upon work supported by the National Science Foundation under VTEPSCoR grants EPS-1101317, EPS-IIA1330446, and OIA 1556770. Any opinions, findings, and conclusions or recommendations expressed in this material are those of the authors and do not necessarily reflect the views of the National Science Foundation or Vermont EPSCoR. We appreciate thoughtful reviews from Ishi Buffam and two anonymous reviewers that greatly improved this work. We thank Joshua Benes, Samuel Parker, Allison Jerram, Brian Pellerin, Richard Rowland, Catherine Winters, Kristen Underwood, Scott Hamshaw, and Donna Rizzo for their helpful contributions to this work. Any use of trade, firm, or product names is for descriptive purposes only and does not imply endorsement by the U.S. Government. The data used in this publication are freely available on HydroShare (<https://goo.gl/R5u3HR>).

References

- Aitkenhead-Peterson, J. A., M. K. Steele, N. Nahar, and K. Santhy (2009), Dissolved organic carbon and nitrogen in urban and rural watersheds of south-central Texas: Land use and land management influences, *Biogeochemistry*, 96(1–3), 119–129, doi:10.1007/s10533-009-9348-2.
- Andrea, B., G. Francesc, L. Jérôme, V. Eusebi, and S. Francesc (2006), Cross-site comparison of variability of DOC and Nitrate c–q hysteresis during the autumn–winter period in three Mediterranean headwater streams: A synthetic approach, *Biogeochemistry*, 77(3), 327–349, doi:10.1007/s10533-005-0711-7.
- Arnold, J. G., P. M. Allen, R. Muttiah, and G. Bernhardt (1995), Automated base-flow separation and recession analysis techniques, *Ground Water*, 33(6), 1010–1018, doi:10.1111/j.1745-6584.1995.tb00046.x.
- Avagyan, A., B. R. K. Runkle, and L. Kutzbach (2014), Application of high-resolution spectral absorbance measurements to determine dissolved organic carbon concentration in remote areas, *J. Hydrol.*, 517, 435–446, doi:10.1016/j.jhydrol.2014.05.060.
- Baker, J. P., et al. (1996), Episodic acidification of small streams in the Northeastern United States: Effects on fish populations, *Ecol. Appl.*, 6(2), 422–437, doi:10.2307/2269380.
- Bierzoza, M. Z., and A. L. Heathwaite (2015), Seasonal variation in phosphorus concentration–discharge hysteresis inferred from high-frequency in situ monitoring, *J. Hydrol.*, 524, 333–347, doi:10.1016/j.jhydrol.2015.02.036.
- Boesch, D. F., R. B. Brinsfield, and R. E. Magnien (2001), Chesapeake Bay eutrophication: Scientific understanding, ecosystem restoration, and challenges for agriculture, *J. Environ. Qual.*, 30(2), 303–320.
- Bowes, M. J., J. T. Smith, and C. Neal (2009), The value of high-resolution nutrient monitoring: A case study of the River Frome, Dorset, UK, *J. Hydrol.*, 378(1–2), 82–96, doi:10.1016/j.jhydrol.2009.09.015.
- Bowes, M. J., H. P. Jarvie, S. J. Halliday, R. A. Skeffington, A. J. Wade, M. Loewenthal, E. Gozzard, J. R. Newman, and E. J. Palmer-Felgate (2015), Characterising phosphorus and nitrate inputs to a rural river using high-frequency concentration–flow relationships, *Sci. Total Environ.*, 511, 608–620, doi:10.1016/j.scitotenv.2014.12.086.
- Boyer, E., C. Goodale, N. Jaworski, and R. Howarth (2002), Anthropogenic nitrogen sources and relationships to riverine nitrogen export in the northeastern U.S.A., *Biogeochemistry*, 57–58(1), 137–169, doi:10.1023/A:1015709302073.
- Boyer, E. W., G. M. Hornberger, K. E. Bencala, and D. M. McKnight (1997), Response characteristics of DOC flushing in an alpine catchment, *Hydro. Processes*, 11(12), 1635–1647.
- Brown, V. A., J. J. McDonnell, D. A. Burns, and C. Kendall (1999), The role of event water, a rapid shallow flow component, and catchment size in summer stormflow, *J. Hydrol.*, 217(3–4), 171–190, doi:10.1016/S0022-1694(98)00247-9.
- Buffam, I., J. N. Galloway, L. K. Blum, and K. J. McGlathery (2001), A stormflow/baseflow comparison of dissolved organic matter concentrations and bioavailability in an Appalachian stream, *Biogeochemistry*, 53(3), 269–306, doi:10.1023/A:1010643432253.

- Bukaveckas, P. A., and M. Robbins-Forbes (2000), Role of dissolved organic carbon in the attenuation of photosynthetically active and ultraviolet radiation in Adirondack lakes, *Freshwater Biol.*, *43*(3), 339–354, doi:10.1046/j.1365-2427.2000.00518.x.
- Butturini, A., M. Alvarez, S. Bernal, E. Vazquez, and F. Sabater (2008), Diversity and temporal sequences of forms of DOC and NO₃-discharge responses in an intermittent stream: Predictable or random succession?, *J. Geophys. Res.*, *113*, G03016, doi:10.1029/2008JG000721.
- Camargo, J. A., and Á. Alonso (2006), Ecological and toxicological effects of inorganic nitrogen pollution in aquatic ecosystems: A global assessment, *Environ. Int.*, *32*(6), 831–849, doi:10.1016/j.envint.2006.05.002.
- Carey, R. O., W. M. Wollheim, G. K. Mulukutla, and M. M. Mineau (2014), Characterizing storm-event nitrate fluxes in a fifth order suburbanizing watershed using in situ sensors, *Environ. Sci. Technol.*, *48*(14), 7756–7765, doi:10.1021/es500252j.
- Carpenter, S. R., N. F. Caraco, D. L. Correll, R. W. Howarth, A. N. Sharpley, and V. H. Smith (1998), Nonpoint pollution of surface waters with phosphorus and nitrogen, *Ecol. Appl.*, *8*(3), 559–568, doi:10.1890/1051-0761(1998)008[0559:NPOSWW]2.0.CO;2.
- Caverly, E., J. M. Kaste, G. S. Hancock, and R. M. Chambers (2013), Dissolved and particulate organic carbon fluxes from an agricultural watershed during consecutive tropical storms, *Geophys. Res. Lett.*, *40*, 5147–5152, doi:10.1002/grl.50982.
- Chanat, J. G., K. C. Rice, and G. M. Hornberger (2002), Consistency of patterns in concentration-discharge plots, *Water Resour. Res.*, *38*(8), doi:10.1029/2001WR000971.
- Chow, A. T., R. A. Dahlgren, and J. A. Harrison (2007), Watershed sources of disinfection byproduct precursors in the Sacramento and San Joaquin Rivers, California, *Environ. Sci. Technol.*, *41*(22), 7645–7652, doi:10.1021/es070621t.
- Creed, I. F., and L. E. Band (1998), Export of nitrogen from catchments within a temperate forest: Evidence for a unifying mechanism regulated by variable source area dynamics, *Water Resour. Res.*, *34*(11), 3105–3120, doi:10.1029/98WR01924.
- Dalzell, B. J., T. R. Filley, and J. M. Harbor (2005), Flood pulse influences on terrestrial organic matter export from an agricultural watershed, *J. Geophys. Res.*, *110*, G02011, doi:10.1029/2005JG000043.
- Darwiche-Criado, N., F. A. Comin, R. Sorando, and J. M. Sanchez-Perez (2015), Seasonal variability of NO₃-mobilization during flood events in a Mediterranean catchment: The influence of intensive agricultural irrigation, *Agric. Ecosyst. Environ.*, *200*, 208–218, doi:10.1016/j.agee.2014.11.002.
- Dhillon, G. S., and S. Inamdar (2013), Extreme storms and changes in particulate and dissolved organic carbon in runoff: Entering uncharted waters?, *Geophys. Res. Lett.*, *40*, 1322–1327, doi:10.1002/grl.50306.
- Dinnes, D. L., D. L. Karlen, D. B. Jaynes, T. C. Kaspar, J. L. Hatfield, T. S. Colvin, and C. A. Cambardella (2002), Nitrogen management strategies to reduce nitrate leaching in tile-drained Midwestern soils, *Agron. J.*, *94*, 153–171, doi:10.2134/agronj2002.1530.
- Donn, M. J., O. V. Barron, and A. D. Barr (2012), Identification of phosphorus export from low-runoff yielding areas using combined application of high frequency water quality data and MODHMS modelling, *Sci. Total Environ.*, *426*, 264–271, doi:10.1016/j.scitotenv.2012.03.021.
- Driscoll, C. T., R. D. Fuller, and D. M. Simone (1988), Longitudinal variations in trace-metal concentrations in a northern forested ecosystem, *J. Environ. Qual.*, *17*(1), 101–107.
- Driscoll, C. T., G. B. Lawrence, A. J. Bulger, T. J. Butler, C. S. Cronan, C. Eagar, K. F. Lambert, G. E. Likens, J. L. Stoddard, and K. C. Weathers (2001), Acidic deposition in the Northeastern United States: Sources and inputs, ecosystem effects, and management strategies, *BioScience*, *51*(3), 180–198, doi:10.1641/0006-3568(2001)051[0180:ADITNU]2.0.CO;2.
- Driscoll, C. T., et al. (2003), Nitrogen pollution in the Northeastern United States: Sources, effects, and management options, *BioScience*, *53*(4), 357–374, doi:10.1641/0006-3568(2003)053[0357:NPITNU]2.0.CO;2.
- Elmore, A. J., and S. S. Kaushal (2008), Disappearing headwaters: Patterns of stream burial due to urbanization, *Frontiers Ecol. Environ.*, *6*(6), 308–312, doi:10.1890/070101.
- Etheridge, J. R., F. Birgand, J. A. Osborne, C. L. Osburn, M. R. Burchell II, and J. Irving (2014), Using in situ ultraviolet-visual spectroscopy to measure nitrogen, carbon, phosphorus, and suspended solids concentrations at a high frequency in a brackish tidal marsh, *Limnol. Oceanogr. Methods*, *12*, 10–22, doi:10.4319/lom.2014.12.10.
- Evans, C., and T. D. Davies (1998), Causes of concentration/discharge hysteresis and its potential as a tool for analysis of episode hydrochemistry, *Water Resour. Res.*, *34*(1), 129–137, doi:10.1029/97WR01881.
- Fellman, J. B., E. Hood, R. T. Edwards, and D. V. D'Amore (2009), Changes in the concentration, biodegradability, and fluorescent properties of dissolved organic matter during stormflows in coastal temperate watersheds, *J. Geophys. Res.*, *114*, G01021, doi:10.1029/2008JG000790.
- Goodale, C. L., S. A. Thomas, G. Fredriksen, E. M. Elliott, K. M. Flinn, T. J. Butler, and M. T. Walter (2009), Unusual seasonal patterns and inferred processes of nitrogen retention in forested headwaters of the Upper Susquehanna River, *Biogeochemistry*, *93*(3), 197–218, doi:10.2307/40647938.
- Groffman, P. M., N. J. Boulware, W. C. Zipperer, R. V. Pouyat, L. E. Band, and M. F. Colosimo (2002), Soil nitrogen cycle processes in urban riparian zones, *Environ. Sci. Technol.*, *36*(21), 4547–4552.
- Hatfield, J., J. Prueger, and D. Jaynes (1998), Environmental impacts of agricultural drainage in the Midwest, in *Proceedings of the 7th Annual Drainage Symposium*, pp. 28–35, Am. Soc. of Agric. Eng., St. Joseph, Mich.
- Helms, J. R., A. Stubbins, J. D. Ritchie, E. C. Minor, D. J. Kieber, and K. Mopper (2008), Absorption spectral slopes and slope ratios as indicators of molecular weight, source, and photobleaching of chromophoric dissolved organic matter, *Limnol. Oceanogr.*, *53*(3), 955–969, doi:10.4319/lo.2008.53.3.0955.
- Hood, E., M. N. Gooseff, and S. L. Johnson (2006), Changes in the character of stream water dissolved organic carbon during flushing in three small watersheds, Oregon, *J. Geophys. Res.*, *111*, G01007, doi:10.1029/2005JG000082.
- House, W. A., and M. S. Warwick (1998), Hysteresis of the solute concentration/discharge relationship in rivers during storms, *Water Res.*, *32*(8), 2279–2290, doi:10.1016/S0043-1354(97)00473-9.
- Inamdar, S., S. Singh, S. Dutta, D. Levia, M. Mitchell, D. Scott, H. Bais, and P. McHale (2011), Fluorescence characteristics and sources of dissolved organic matter for stream water during storm events in a forested mid-Atlantic watershed, *J. Geophys. Res.*, *116*, G03043, doi:10.1029/2011JG001735.
- Inamdar, S. P., N. O'Leary, M. J. Mitchell, and J. T. Riley (2006), The impact of storm events on solute exports from a glaciated forested watershed in western New York, USA, *Hydrol. Processes*, *20*(16), 3423–3439, doi:10.1002/hyp.6141.
- Johnson, F. A., and J. W. East (1982), Cyclical relationships between river discharge and chemical concentration during flood events, *J. Hydrol.*, *57*(1), 93–106, doi:10.1016/0022-1694(82)90105-6.
- Johnson, K. S., and L. J. Coletti (2002), In situ ultraviolet spectrophotometry for high resolution and long-term monitoring of nitrate, bromide and bisulfide in the ocean, *Deep Sea Res., Part I*, *49*(7), 1291–1305, doi:10.1016/S0967-0637(02)00020-1.
- Kaushal, S. S., and K. T. Belt (2012), The urban watershed continuum: Evolving spatial and temporal dimensions, *Urban Ecosyst.*, *15*(2), 409–435, doi:10.1007/s11252-012-0226-7.

- Kaushal, S. S., P. M. Groffman, L. E. Band, C. A. Shields, R. P. Morgan, M. A. Palmer, K. T. Belt, C. M. Swan, S. E. G. Findlay, and G. T. Fisher (2008), Interaction between urbanization and climate variability amplifies watershed nitrate export in Maryland, *Environ. Sci. Technol.*, 42(16), 5872–5878, doi:10.1021/es800264f.
- Kominoski, J. S., and A. D. Rosemond (2011), Conservation from the bottom up: Forecasting effects of global change on dynamics of organic matter and management needs for river networks, *Freshwater Sci.*, 31(1), 51–68, doi:10.1899/10-160.1.
- Kraus, T. E. C., B. A. Bergamaschi, P. J. Hernes, R. G. M. Spencer, R. Stepanauskas, C. Kendall, R. F. Losee, and R. Fujii (2008), Assessing the contribution of wetlands and subsided islands to dissolved organic matter and disinfection byproduct precursors in the Sacramento–San Joaquin River Delta: A geochemical approach, *Org. Geochem.*, 39(9), 1302–1318, doi:10.1016/j.orggeochem.2008.05.012.
- Kruskal, W. H., and W. A. Wallis (1952), Use of ranks in one-criterion variance analysis, *J. Am. Stat. Assoc.*, 47(260), 583–621, doi:10.2307/2280779.
- Langergraber, G., N. Fleischmann, and F. Hofstadter (2003), A multivariate calibration procedure for UV/VIS spectrometric quantification of organic matter and nitrate in wastewater, *Water Sci. Technol.*, 47(2), 63–71.
- Levene, H. (1960), Robust tests for equality of variances, in *Contributions to Probability and Statistics: Essays in Honor of Harold Hotelling*, edited by I. Olkin, pp. 278–292, Stanford Univ. Press, Stanford, Calif.
- Likens, G. E. (2013), *Biogeochemistry of a Forested Ecosystem*, 3rd ed., 208 pp., Springer, New York.
- Lloyd, C. E. M., J. E. Freer, P. J. Johnes, and A. L. Collins (2016), Technical Note: Testing an improved index for analysing storm discharge–concentration hysteresis, *Hydrol. Earth Syst. Sci.*, 20(2), 625–632, doi:10.5194/hess-20-625-2016.
- McGlynn, B. L., and J. J. McDonnell (2003), Quantifying the relative contributions of riparian and hillslope zones to catchment runoff, *Water Resour. Res.*, 39(11), 1310, doi:10.1029/2003WR002091.
- Mevik, B., R. Wehrens, and K. H. Liland (2016), *pls: Least Squares and Principal Component Regression*, R package version 2.6-0. [Available at <https://CRAN.R-project.org/package=pls>.]
- Moore, R. D. (2005), Slug injection using salt in solution, *Streamline Watershed Manage. Bull.*, 8(2), 1–6.
- Moore, T. R., and R. J. Jackson (1989), Dynamics of dissolved organic carbon in forested and disturbed catchments, Westland, New Zealand: 2. Larry River, *Water Resour. Res.*, 25(6), 1331–1339, doi:10.1029/WR025i006p01331.
- Morel, B., P. Durand, A. Jaffrezic, G. Gruau, and J. Molenat (2009), Sources of dissolved organic carbon during stormflow in a headwater agricultural catchment, *Hydrol. Processes*, 23(20), 2888–2901, doi:10.1002/hyp.7379.
- Morris, D. P., H. Zagarese, C. E. Williamson, E. G. Balseiro, B. R. Hargreaves, B. Modenutti, R. Moeller, and C. Queimalinos (1995), The attenuation of solar UV radiation in lakes and the role of dissolved organic carbon, *Limnol. Oceanogr.*, 40(8), 1381–1391.
- Newcomer, T. A., S. S. Kaushal, P. M. Mayer, A. R. Shields, E. A. Canuel, P. M. Groffman, and A. J. Gold (2012), Influence of natural and novel organic carbon sources on denitrification in forest, degraded urban, and restored streams, *Ecol. Monogr.*, 82(4), 449–466, doi:10.1890/12-0458.1.
- Nguyen, H. V.-M., M.-H. Lee, J. Hur, and M. A. Schlautman (2013), Variations in spectroscopic characteristics and disinfection byproduct formation potentials of dissolved organic matter for two contrasting storm events, *J. Hydrol.*, 481, 132–142, doi:10.1016/j.jhydrol.2012.12.044.
- Oeurng, C., S. Sauvage, and J.-M. Sánchez-Pérez (2010), Temporal variability of nitrate transport through hydrological response during flood events within a large agricultural catchment in south-west France, *Sci. Total Environ.*, 409(1), 140–149, doi:10.1016/j.scitotenv.2010.09.006.
- Outram, F. N., et al. (2014), High-frequency monitoring of nitrogen and phosphorus response in three rural catchments to the end of the 2011–2012 drought in England, *Hydrol. Earth Syst. Sci.*, 18(9), 3429–3448, doi:10.5194/hess-18-3429-2014.
- Pardo, L. H., et al. (2011), Effects of nitrogen deposition and empirical nitrogen critical loads for ecoregions of the United States, *Ecol. Appl.*, 21(8), 3049–3082, doi:10.1890/10-2341.1.
- Parr, T. B., C. S. Cronan, T. Ohno, S. E. G. Findlay, S. M. C. Smith, and K. S. Simon (2015), Urbanization changes the composition and bioavailability of dissolved organic matter in headwater streams, *Limnol. Oceanogr.*, 60, 885–900, doi:10.1002/lno.10060.
- Paternoster, R., R. Brame, P. Mazerolle, and A. Piquero (1998), Using the correct statistical test for the equality of regression coefficients, *Criminology*, 36(4), 859–866, doi:10.1111/j.1745-9125.1998.tb01268.x.
- Pellerin, B. A., J. F. Saraceno, J. B. Shanley, S. D. Sebestyen, G. R. Aiken, W. M. Wollheim, and B. A. Bergamaschi (2012), Taking the pulse of snowmelt: In situ sensors reveal seasonal, event and diurnal patterns of nitrate and dissolved organic matter variability in an upland forest stream, *Biogeochemistry*, 108(1), 183–198, doi:10.1007/s10533-011-9589-8.
- Prairie, Y. T. (2008), Carbocentric limnology: Looking back, looking forward, *Can. J. Fish. Aquat. Sci.*, 65(3), 543–548, doi:10.1139/f08-011.
- R Core Team (2015), *R: A Language and Environment for Statistical Computing*, R Found. for Stat. Comput., Vienna.
- Ravichandran, M. (2004), Interactions between mercury and dissolved organic matter—A review, *Chemosphere*, 55(3), 319–331, doi:10.1016/j.chemosphere.2003.11.011.
- Raymond, P., and J. Saiers (2010), Event controlled DOC export from forested watersheds, *Biogeochemistry*, 100(1–3), 197–209, doi:10.1007/s10533-010-9416-7.
- Reckhow, D. A., and P. C. Singer (1990), Chlorination by-products in drinking waters—From formation potentials to finished water concentrations, *J. Am. Water Works Assoc.*, 82(4), 173–180.
- Rosenzweig, B. R., H. S. Moon, J. A. Smith, M. L. Baeck, and P. R. Jaffe (2008), Variation in the instream dissolved inorganic nitrogen response between and within rainstorm events in an urban watershed, *J. Environ. Sci. Health, Part A*, 43(11), 1223–1233, doi:10.1080/10934520802225190.
- Royer, T. V., and M. B. David (2005), Export of dissolved organic carbon from agricultural streams in Illinois, USA, *Aquat. Sci.*, 67(4), 465–471, doi:10.1007/s00027-005-0781-6.
- Royer, T. V., M. B. David, and L. E. Gentry (2006), Timing of riverine export of nitrate and phosphorus from agricultural watersheds in Illinois: Implications for reducing nutrient loading to the Mississippi River, *Environ. Sci. Technol.*, 40(13), 4126–4131, doi:10.1021/es052573n.
- Rusjan, S., M. Brilly, and M. Mikoš (2008), Flushing of nitrate from a forested watershed: An insight into hydrological nitrate mobilization mechanisms through seasonal high-frequency stream nitrate dynamics, *J. Hydrol.*, 354(1–4), 187–202, doi:10.1016/j.jhydrol.2008.03.009.
- Sanchez, C. A., and A. M. Blackmer (1988), Recovery of anhydrous ammonia-derived nitrogen-15 during three years of corn production in Iowa, *Agron. J.*, 80, 102–108, doi:10.2134/agronj1988.00021962008000010023x.
- Saraceno, J. F., B. A. Pellerin, B. D. Downing, E. Boss, P. A. M. Bachand, and B. A. Bergamaschi (2009), High-frequency in situ optical measurements during a storm event: Assessing relationships between dissolved organic matter, sediment concentrations, and hydrologic processes, *J. Geophys. Res.*, 114, G00F09, doi:10.1029/2009JG000989.
- Sebestyen, S. D., J. B. Shanley, E. W. Boyer, C. Kendall, and D. H. Doctor (2014), Coupled hydrological and biogeochemical processes controlling variability of nitrogen species in streamflow during autumn in an upland forest, *Water Resour. Res.*, 50, 1569–1591, doi:10.1002/2013WR013670.

- Sickman, J. O., M. J. Zanol, and H. L. Mann (2007), Effects of urbanization on organic carbon loads in the Sacramento River, California, *Water Resour. Res.*, *43*, W11422, doi:10.1029/2007WR005954.
- Sivirichi, G. M., S. S. Kaushal, P. M. Mayer, C. Welty, K. T. Belt, T. A. Newcomer, K. D. Newcomb, and M. M. Grese (2011), Longitudinal variability in streamwater chemistry and carbon and nitrogen fluxes in restored and degraded urban stream networks, *J. Environ. Monit.*, *13*(2), 288–303, doi:10.1039/C0EM00055H.
- Smith, V. H., G. D. Tilman, and J. C. Nekola (1999), Eutrophication: Impacts of excess nutrient inputs on freshwater, marine, and terrestrial ecosystems, *Environ. Pollut.*, *100*(1–3), 179–196, doi:10.1016/S0269-7491(99)00091-3.
- Sobczak, W., S. Findlay, and S. Dye (2003), Relationships between DOC bioavailability and nitrate removal in an upland stream: An experimental approach, *Biogeochemistry*, *62*(3), 309–327, doi:10.1023/A:1021192631423.
- Stanley, E. H., S. M. Powers, N. R. Lottig, I. Buffam, and J. T. Crawford (2012), Contemporary changes in dissolved organic carbon (DOC) in human-dominated rivers: Is there a role for DOC management?, *Freshwater Biol.*, *57*, 26–42, doi:10.1111/j.1365-2427.2011.02613.x.
- Stubbins, A., J. F. Lapierre, M. Berggren, Y. T. Prairie, T. Dittmar, and P. A. del Giorgio (2014), What's in an EEM? Molecular signatures associated with dissolved organic fluorescence in Boreal Canada, *Environ. Sci. Technol.*, *48*(18), 10,598–10,606, doi:10.1021/es502086e.
- Townsend, A. R., et al. (2003), Human health effects of a changing global nitrogen cycle, *Frontiers Ecol. Environ.*, *1*(5), 240–246, doi:10.1890/1540-9295(2003)001[0240:HHEOAC]2.0.CO;2.
- Turnipseed, D. P., and V. B. Sauer (2010), Discharge measurements at gaging stations, *Rep. 2328–7055*, U.S. Geol. Surv., Reston, Va.
- Van Herpe, Y., and P. A. Troch (2000), Spatial and temporal variations in surface water nitrate concentrations in a mixed land use catchment under humid temperate climatic conditions, *Hydrol. Processes*, *14*(14), 2439–2455, doi:10.1002/1099-1085(20001015)14:14 < 2439::AID-HYP105 > 3.0.CO;2-H.
- Vidon, P., L. E. Wagner, and E. Soyeux (2008), Changes in the character of DOC in streams during storms in two Midwestern watersheds with contrasting land uses, *Biogeochemistry*, *88*(3), 257–270, doi:10.1007/s10533-008-9207-6.
- Walford, N. (2011), *Practical Statistics for Geographers and Earth Scientists*, vol. xxiii, 416 pp., Wiley-Blackwell, Oxford, U. K.
- Walsh, C. J., A. H. Roy, J. W. Feminella, P. D. Cottingham, P. M. Groffman, and R. P. Morgan (2005), The urban stream syndrome: Current knowledge and the search for a cure, *J. North Am. Benthol. Soc.*, *24*(3), 706–723, doi:10.1899/04-028.1.
- Walsh, J., et al. (2014), Climate change impacts in the United States: The third national climate assessment, report, 19–67 pp., U.S. Global Change Res. Program, Washington, D. C., doi:10.7930/J0KW5CXT.
- Webster, J. R., J. D. Newbold, S. A. Thomas, H. M. Valett, and P. J. Mulholland (2009), Nutrient uptake and mineralization during leaf decay in streams—A model simulation, *Int. Rev. Hydrobiol.*, *94*(4), 372–390, doi:10.1002/iroh.200811158.
- Wilson, H., and M. Xenopoulos (2008), Ecosystem and seasonal control of stream dissolved organic carbon along a gradient of land use, *Ecosystems*, *11*(4), 555–568, doi:10.1007/s10021-008-9142-3.
- Wilson, H. F., and M. A. Xenopoulos (2009), Effects of agricultural land use on the composition of fluvial dissolved organic matter, *Nat. Geosci.*, *2*(1), 37–41.
- Winchell, M., D. Meals, S. Folle, J. Moore, D. Braun, C. DeLeo, K. Budreski, and R. Schiff (2011), Identification of critical source areas of phosphorus within the Vermont sector of the Missisquoi Bay Basin, *Tech. Rep. 63 B*, Lake Champlain Basin Program, Grand Isle, Vt.
- Yoon, B., and P. A. Raymond (2012), Dissolved organic matter export from a forested watershed during Hurricane Irene, *Geophys. Res. Lett.*, *39*, L18402, doi:10.1029/2012GL052785.
- Zhang, Z., T. Fukushima, Y. Onda, T. Gomi, T. Fukuyama, R. Sidle, K. Kosugi, and K. Matsushige (2007), Nutrient runoff from forested watersheds in central Japan during typhoon storms: Implications for understanding runoff mechanisms during storm events, *Hydrol. Processes*, *21*(9), 1167–1178, doi:10.1002/hyp.6677.